



THE UNIVERSITY *of* EDINBURGH

## Edinburgh Research Explorer

### Photocatalytic degradation of bisphenol-A under UV-LED, blacklight and solar irradiation

**Citation for published version:**

Davididou, K, Nelson, R, monteagudo, JM, Duran, A, Exposito, A & Chatzisyneon, E 2018, 'Photocatalytic degradation of bisphenol-A under UV-LED, blacklight and solar irradiation', *Journal of Cleaner Production*, vol. 203, pp. 13-21. <https://doi.org/10.1016/j.jclepro.2018.08.247>

**Digital Object Identifier (DOI):**

[10.1016/j.jclepro.2018.08.247](https://doi.org/10.1016/j.jclepro.2018.08.247)

**Link:**

[Link to publication record in Edinburgh Research Explorer](#)

**Document Version:**

Peer reviewed version

**Published In:**

Journal of Cleaner Production

**General rights**

Copyright for the publications made accessible via the Edinburgh Research Explorer is retained by the author(s) and / or other copyright owners and it is a condition of accessing these publications that users recognise and abide by the legal requirements associated with these rights.

**Take down policy**

The University of Edinburgh has made every reasonable effort to ensure that Edinburgh Research Explorer content complies with UK legislation. If you believe that the public display of this file breaches copyright please contact [openaccess@ed.ac.uk](mailto:openaccess@ed.ac.uk) providing details, and we will remove access to the work immediately and investigate your claim.



**Photocatalytic degradation of bisphenol-A under UV-LED, blacklight and solar  
irradiation**

K. Davididou<sup>a</sup>, R. Nelson<sup>a</sup>, J. M. Monteagudo<sup>b</sup>, A. Durán<sup>b</sup>, A. J. Expósito<sup>b</sup>, E.  
Chatzisyneon<sup>a,\*</sup>

<sup>a</sup> School of Engineering, Institute for Infrastructure and Environment, The University  
of Edinburgh, Edinburgh EH9 3JL, United Kingdom.

<sup>b</sup> Department of Chemical Engineering, Grupo IMAES, Escuela Técnica Superior de  
Ingenieros Industriales, Instituto de Investigaciones Energéticas y Aplicaciones  
Industriales (INEI), University of Castilla-La Mancha, Avda. Camilo José Cela 3,  
13071 Ciudad Real, Spain.

\*Corresponding author: E-mail: e.chatzisyneon@ed.ac.uk; Tel.: +44 1316505711

## Abstract

This study aims at investigating the photocatalytic treatment of bisphenol-A (BPA) under various irradiation sources in order to identify cleaner and more sustainable technologies compared to conventional photocatalytic wastewater treatment systems. For this purpose, parallel experimental runs were carried out in two batch-operated slurry photoreactors under UVA irradiation provided by either a light-emitting diode (UV-LED) or a UV blacklight lamp (UV-BL), as well as in a solar compound parabolic collector (CPC) reactor under natural sunlight. The effect of key operating parameters, such as the initial BPA and  $\text{TiO}_2$  concentrations, water matrix, and treatment time, on the efficiency of the three photocatalytic systems was evaluated. The photocatalytic degradation of BPA was found to fit well with the pseudo-first-order kinetic model. BPA removal rate increased with catalyst concentration and with decreasing the initial concentration of BPA. The addition of humic acids was found to be inhibitory for all photocatalytic systems. At the best conditions assayed ( $C_0 = 2.5$  mg/L,  $\text{TiO}_2 = 250$  mg/L), BPA was completely degraded within 20, 30, and 120 min under UV-LED, solar, and UV-BL irradiation, respectively. The corresponding reaction rates were 0.230, 0.151, and  $0.025 \text{ min}^{-1}$ , and TOC removal was 88, 67, and 33% after 90 min of treatment. In all cases,  $\text{TiO}_2/\text{UV-LED}$  achieved the highest removal efficiency and it was found to be significantly more energy-efficient than the  $\text{TiO}_2/\text{UV-BL}$  system. All in all, LED-driven photocatalysis was found to be advantageous over conventional  $\text{TiO}_2/\text{UV-BL}$  systems in terms of performance and sustainability, and an appropriate alternative to solar photocatalysis in areas where sunlight is inadequate.

**Keywords:** EDCs; water purification; emerging contaminants; light-emitting diodes; solar CPC; photocatalysis

## **1 Introduction**

Bisphenol-A (BPA), a well-known endocrine disrupting compound (EDC), is an alkylphenol used extensively in the synthesis of polycarbonate polymers and epoxy resins (Deblonde et al., 2011). Due to its heat resistance and elasticity, BPA is found in several products, such as food containers, metal cans, and baby bottles (Giulivo et al., 2016; Rubin, 2011). Changes of the inner temperature and pH of BPA-containing materials result in hydrolysis of the ester bonds of BPA, which subsequently lead to BPA leaching into foods and beverages. Ingested BPA is thought to be absorbed by the gastrointestinal tract and then excreted in urine (Giulivo et al., 2016). Existing conventional wastewater treatment plants (WWTPs) are not typically designed for the treatment of such persistent compounds (Belgiorno et al., 2007; Luo et al., 2014), and therefore BPA escapes intact into the aquatic environment by means of the effluent discharges of WWTPs. As a result, BPA has been extensively detected in influent and effluent of WWTPs, groundwater, surface, and drinking water (Kasprzyk-Hordern et al., 2009; Kleywegt et al., 2011; Loos et al., 2010). Exposure to BPA, even at trace level concentrations, has been found to affect the reproductive system of humans (Li et al., 2010; Meeker et al., 2010), and has been linked to growth, developmental, and reproductive effects on aquatic invertebrates, fishes, amphibians, reptiles, birds, and mammalian wildlife (Flint et al., 2012; Zhang et al., 2016). To this end, new, effective and sustainable treatment methods are required to set a barrier to the release of emerging microcontaminants, such as BPA, into the environment.

1 TiO<sub>2</sub>-mediated photocatalysis has received considerable attention because of its  
2 efficiency to eliminate EDCs in water and wastewater (Belgiorno et al., 2007;  
3 Dalrymple et al., 2007). Photocatalytic oxidation is initiated upon ultraviolet (UV)  
4 illumination of a catalyst, usually TiO<sub>2</sub>. Highly reactive species, mainly hydroxyl  
5 radicals (<sup>•</sup>OH), are then formed and attack organic pollutants, which are eventually  
6 mineralised into CO<sub>2</sub> and inorganic anions (Herrmann, 1999; Malato et al., 2009).  
7 Sunlight is a free and plentiful renewable energy that can be also used as an  
8 irradiation source to increase process sustainability (Legrini et al., 1993). Solar  
9 photocatalysis takes advantage of the near-UV band of the solar spectrum to excite  
10 TiO<sub>2</sub> catalysts (Malato et al., 2009). In areas where sunlight is inadequate, artificial  
11 irradiation is required for photon generation to supplement the efficiency of  
12 traditionally employed conventional blacklight fluorescent (UV-BL) lamps (Tokode  
13 et al., 2015). However UV-BL lamps suffer from several drawbacks, such as their low  
14 energy efficiency, short lifespan and health and safety issues since they contain toxic  
15 mercury gas (Jo and Tayade, 2014). As a consequence, UV-BL photocatalytic  
16 applications suffer from high treatment costs and increased environmental impacts  
17 (Chatzisyneon et al., 2013; Mahamuni and Adewuyi, 2010). To date, 128 countries  
18 have signed the Minamata Convention on Mercury, which aims at the gradual phase-  
19 out of mercury-containing products by 2020 (Matafonova and Batoev, 2018).  
20 Therefore, sustainable mercury-free UV sources are sought to power photochemical  
21 oxidation technologies. In this regard, UV light-emitting diodes (UV-LEDs) can be  
22 used as eco-friendly alternatives to UV-BL lamps (Davididou et al., 2018). Key  
23 features of LEDs include energy efficiency, extended lifetime, and toxic-free nature  
24 (i.e. free of mercury and lead, and absence of gas fill) that can lower the cost and  
25 improve process sustainability (Tokode et al., 2015).

1 Several studies have dealt with the photocatalytic degradation of BPA under  
2 conventional UVA, vis-LED, and solar irradiation (Subagio et al., 2010; Tsai et al.,  
3 2009; Zacharakis et al., 2013). (Saggioro et al., 2014) compared the removal  
4 efficiency of BPA under conventional UVA and solar irradiation in batch and  
5 compound parabolic collector (CPC) reactors using TiO<sub>2</sub> P25 suspensions. The  
6 authors reported enhanced photocatalytic performance in the solar CPC compared to  
7 the batch reactor, ascribing it to the optimized optical design of CPC, which allows  
8 the use of both direct and diffuse solar irradiation. The present study investigates the  
9 photocatalytic degradation of BPA under UVA irradiation provided by either a UV-  
10 LED, UV-BL or natural sunlight in parallel experimental runs. To the best of the  
11 authors' knowledge, this is the first time that the efficiency of three different  
12 photocatalytic systems is compared under similar experimental conditions (i.e.  
13 catalyst concentration, substrate concentration, water matrix). Results of this work  
14 will create important scientific knowledge on the kinetic rates of BPA degradation  
15 under several irradiation sources and how these can be affected by altering basic  
16 operating parameters. The lack of an environmentally friendly and low-cost  
17 irradiation source with constant availability of light is the main technical barrier that  
18 impedes the large-scale application of TiO<sub>2</sub>-mediated photocatalytic water treatment.  
19 Therefore, findings of this work can be used as a tool for researchers and water  
20 industry to further scale-up the process by using the most suitable irradiation source  
21 (or a combination of them) that will enable an effective and sustainable treatment of  
22 water and wastewater. Moreover, to the best of the authors' knowledge, degradation  
23 of BPA under UVA-LED irradiation in the presence of TiO<sub>2</sub> P25 suspensions has not  
24 been reported in the literature yet.

1 For this purpose, photocatalytic experiments were performed both in batch and CPC  
2 reactors in the presence of TiO<sub>2</sub> catalyst. The degradation of BPA was studied with  
3 consideration to the potential application of photocatalysis as a final polishing step  
4 after secondary treatment in domestic wastewater or drinking water treatment plants.  
5 The effect of key operating parameters, such as initial substrate and catalyst  
6 concentration, treatment time, and water matrix on photocatalytic performance was  
7 evaluated. Furthermore, the three photocatalytic systems were compared in terms of  
8 their technical and economic benefits.

## 9 **2 Materials and Methods**

### 10 **2.1 Materials**

11 Bisphenol-A (BPA;  $\geq 99\%$  purity, CAS No. 80-05-7) was purchased from Sigma-  
12 Aldrich. Leonardite humic acid (HA) IHSS standard was used. HA stock solution was  
13 prepared by dissolving a prescribed amount of HA in 0.1 M NaOH and further  
14 diluting it in ultra-pure water (UPW; 18.2 M $\Omega$ .cm at 25 °C, ELGA LabWater).  
15 Aeroxide TiO<sub>2</sub> P25 (anatase:rutile 80:20, 21 nm primary particle size,  $50 \pm 15$  m<sup>2</sup>/g  
16 BET surface area), supplied by Evonik Industries, was used as the catalyst.

17

### 18 **2.2 Photocatalytic experiments**

19 Experiments under artificial irradiation were performed in batch-operated, slurry  
20 photoreactors at lab-scale. For LED-driven photocatalysis, an indium gallium nitride  
21 (InGaN) UVA emitter (UV-LED;  $\lambda = 365$  nm, LZ4-00U600, LED Engin) was  
22 employed providing continuous irradiation. The UVA emitter was mounted onto a  
23 heat sink (588-SV-LED-176E, Ohmite S Series) to prevent radiant flux decrease due  
24 to temperature rise on the diode's surface. The LED assembly was placed above the

1 reactor and a quartz protective plate was placed between them (Figure 1a). The  
2 second irradiation source was a UV low-pressure blacklight fluorescent lamp (UV-  
3 BL; PLS G23, Casell Lighting), emitting predominantly at  $\lambda = 365$  nm. UV-BL was  
4 housed in a quartz tube and, for the sake of comparison, positioned on top of the  
5 reactor at the same height as the LED assembly (i.e. 8 cm distance between irradiation  
6 source and surface of reactant mixture at the beginning of each experiment) (Figure  
7 1b). Both set-ups were covered with aluminium shields to prevent light diffusion out  
8 of the reactors and minimise penetration of ambient light. The reactors (250 mL  
9 Schott Duran beakers, diameter 7 cm, height 9 cm) provided an illuminated area of  
10  $38.5\text{ cm}^2$ . The quartz glasses were UV transparent and used to protect the lamps from  
11 water spills. UV-LED and UV-BL irradiation sources were driven by electrical power  
12 of 11 W and were connected in series to a DC power supply.

13  
14 Figure 1. Schematics of (a) UV-LED, (b) UV-BL, and (c) solar CPC reactors.

15  
16 In a typical run, 150 mL of BPA solution was introduced in the photoreactor and a  
17 prescribed amount of catalyst was added. The obtained slurry solution was  
18 continuously stirred magnetically at 500 rpm to promote uniform dispersion of  
19 catalyst powder and dissolved oxygen. At the beginning of each experiment, the  
20 solution was stirred in the dark for 30 min to ensure complete adsorption-desorption  
21 equilibrium of BPA on the catalyst surface. After adsorption, the UV light source was  
22 switched on (taken as  $t = 0$ ), initiating the photocatalytic redox reactions. Samples  
23 were withdrawn at regular time intervals and filtered through  $0.45\text{ }\mu\text{m}$  polyvinylidene  
24 fluoride (PVDF) syringe filters (CM Scientific Ltd) to remove catalyst particles and



1 further analysed in terms of their organic content. All experiments were conducted at  
2 the inherent pH of BPA solution ( $\sim 6.4$ ), which remained constant during  
3 photocatalytic treatment.

4 The photocatalytic experiments under solar irradiation were carried out in a  
5 compound parabolic collector (CPC) with  $0.25 \text{ m}^2$  total illuminated surface area  
6 (Figure 1c), manufactured by Ecosystem S.A. The CPC reactor consisted of 2  
7 borosilicate tubes providing an irradiated volume of 2 L, solar reflectors (anodised  
8 aluminium with a concentration factor of 1), a continuously stirred tank (1.5 L), a  
9 centrifugal recirculation pump (flow rate = 30 L/min), connecting tubes, and valves.

10 The CPC reactor was mounted on a fixed south-facing platform  $39^\circ$  tilted, which was  
11 installed in Ciudad Real (Spain). A radiometer (Ecosystem, ACADUS 85),  $45^\circ$  tilted,  
12 was used to provide the global (direct + diffuse) UV (200 - 400 nm) radiation data.

13 The light intensity of solar irradiation during the photocatalytic experiments ranged  
14 from 25 to  $30 \text{ W/m}^2$ . At the beginning of each experiment, the BPA-polluted water  
15 matrix and the catalyst were added into the continuously stirred tank and pumped  
16 through the covered reactor for 30 min. This step was applied to ensure adequate  
17 mixing and complete equilibration of adsorption-desorption of BPA onto catalyst  
18 surface. The reactor was then uncovered initiating the photocatalytic redox reactions  
19 (taken as  $t = 0$ ). Samples were withdrawn at predetermined times, filtered and  
20 analysed, as previously described.

21

## 22 **2.3 Analytical techniques**

23 BPA concentration in the filtered water samples was measured by a high performance  
24 liquid chromatography (HPLC) system (S200 Pump, S225 Autosampler, Perkin

Elmer) coupled with a diode array detector (S200 EP, Perkin Elmer). Separation was performed on a reverse phase C18 analytical column (Luna Phenomenex 5u, 250 x 4.6 mm) in isocratic elution mode (flow rate = 1 mL/min). The mobile phase consisted of 35:65 (v/v) UPW:acetonitrile (Frontistis et al., 2011). The injection volume was 40  $\mu$ L and the detection wavelength was set at 225 nm.

Mineralisation efficiency was determined by measuring the residual organic concentration by a TOC analyser (Shimadzu TOC-V<sub>CPH</sub>) in the non-purgeable organic carbon (NPOC) mode.

Light intensity and spectral distribution of UV-LED and UV-BL light sources were acquired by a Labsphere spectral irradiance receiver head (E1000) with a concentrator area of 1 cm<sup>2</sup>. The distance between the receiver head and the irradiation source was set at 8 cm, which was equal to the distance between UV-LED or UV-BL and the surface of the reactant mixture. More information about the analysis can be found in (Tsonev et al., 2015). The spectral irradiance of UV-LED relatively to that of UV-BL can be seen in Figure 2. The light intensities of UV-LED and UV-BL were estimated to be 1005 and 22.49 W/m<sup>2</sup>, respectively.

Figure 2. The relative spectral irradiance of UV-LED and UV-BL irradiation sources and the action spectra of TiO<sub>2</sub> P25 catalyst (in grey).

## 2.4 Energy consumption

The energy consumption of UV-LED and UV-BL light sources was estimated using figures-of-merit, developed to evaluate the energy efficiency of electric-energy-driven advanced oxidation processes. (Bolton et al., 2001) introduced the concept of the

1 electric energy per order,  $E_{EO}$ , defined as the energy required for 90% degradation of  
 2 a pollutant per cubic meter of contaminated water. The  $E_{EO}$  (kWh/m<sup>3</sup>/order) for a  
 3 batch-operated photoreactor is calculated by equation (1):

$$4 \quad E_{EO} = \frac{P \times t \times 1000}{V \times 60 \times \log\left(\frac{C_i}{C_f}\right)} \quad (1)$$

5 where  $P$  (kW) is the power of the irradiation source,  $t$  (min) is the irradiation time,  $V$   
 6 (L) is the volume of the treated effluent, and  $C_i$  and  $C_f$  (mg/L) are the initial and the  
 7 final pollutant concentrations.

8

## 9 **2.5 UV energy requirement**

10 The UV energy requirement of each photocatalytic system is calculated by equation  
 11 (2):

$$12 \quad Q_{UV,n+1} = Q_{UV} + \Delta t_n \cdot \overline{UV}_{G,n+1} \cdot \frac{A_i}{V_T}; \quad \Delta t_n = t_{n+1} - t_n \quad (2)$$

13 where  $Q_{UV}$  (kJ/L) is the accumulated UV energy per unit of volume,  $\overline{UV}_{G,n+1}$  (W/m<sup>2</sup>)  
 14 is the average solar UV radiation ( $\lambda < 400$  nm) measured between  $t_{n+1}$  and  $t_n$ ,  $A_i$   
 15 (m<sup>2</sup>) is the illuminated area, and  $V_T$  (L) is the total volume of the reactor. The  
 16 calculation of  $Q_{UV}$  for the solar CPC reactor was based on the average light intensity  
 17 measured (i.e. 27.5 W/m<sup>2</sup>).

18

### 3 Results and Discussion

#### 3.1 Effect of initial BPA concentration

To assess the effect of the initial concentration of BPA on photocatalytic performance, different initial BPA concentrations (2.5 – 10 mg/L) were applied in the presence of 125 mg/L TiO<sub>2</sub>. As can be seen in Table 1 and the inset graphs of Figure 3, reaction rates decrease with increasing initial concentrations. For instance, a 4-fold increase of BPA concentration (i.e. from 2.5 to 10 mg/L) results in a 3-fold decrease of the reaction rate (i.e. from 0.021 to 0.007 min<sup>-1</sup>) during UV-BL photocatalytic treatment. The fact that reaction rate changes proportionally less than the initial concentration of BPA implies a shift from first- to zero-order kinetics [although the pseudo-first-order kinetic model was found to describe well the photocatalytic degradation of BPA]. The plot of the normalised BPA concentration against irradiation time resulted in straight lines with the coefficient of linear regression of data fitting,  $r^2$ , ranging from 0.90 to 1.00 (Table 1). From the slopes of the resulting lines, the values of the pseudo-first-order kinetic constant,  $k$ , were computed.

The increase of initial BPA concentration resulted in decreased removal efficiencies. In detail, when the initial concentration of BPA increased from 2.5 to 10 mg/L, the degradation rate decreased from 99.9 to 79.7% ( $k = 0.179 - 0.036$  min<sup>-1</sup>) under UV-LED irradiation, and from 66.8 to 29.5% ( $k = 0.021 - 0.007$  min<sup>-1</sup>) under UV-BL irradiation (Figures 3a and 3b). Similarly, the gradual increase of initial BPA concentration (up to 10 mg/L) decreased its removal efficiency from 99.9 to 72.9% ( $k = 0.132 - 0.035$  min<sup>-1</sup>) in the CPC reactor (Figure 3c). It is generally accepted that increase in the initial organic concentration, at a fixed set of photocatalytic conditions, lowers the ratio of oxidant species to substrate molecules and further results in decreased degradation yields (Dimitrakopoulou et al., 2012), thus explaining the

findings presented above. According to the results, TiO<sub>2</sub>/UV-LED and TiO<sub>2</sub>/solar systems could degrade up to 8 and 7.2 mg/L BPA within 45 min of treatment, whereas the respective removal for TiO<sub>2</sub>/UV-BL system was limited to 2.9 mg/L.

Figure 3. Effect of initial BPA concentration on photocatalytic degradation under (a) UV-LED, (b) UV-BL, and (c) solar irradiation. Inset graphs: relationship between reaction rate constant and initial BPA concentration (TiO<sub>2</sub> = 125 mg/L).

Table 1. Removal percentages (R), pseudo-first-order kinetic constants (*k*), and coefficients of linear regression of data fitting (*r*<sup>2</sup>) for the photocatalytic degradation of BPA under UV-LED, UV-BL, and solar irradiation.

### 3.2 Effect of catalyst concentration

Control experiments (i.e. photolysis and catalysis in the dark) were performed to assess the effect of the presence of the catalyst on process efficiency. As can be seen in Figure 4, BPA degradation is negligible after 45 min for both photolysis and catalysis in the dark in TiO<sub>2</sub>/UV-LED and TiO<sub>2</sub>/UV-BL systems, proving that photocatalysis is the main mechanism for BPA removal. The maximum UV absorbance of BPA appears at 199 and 276 nm, therefore BPA cannot be photolyzed by either UV-LED or UV-BL, which both emit predominantly at 365 nm. Furthermore, existence of UV light ( $\lambda < 380$  nm) is a prerequisite for the activation of TiO<sub>2</sub> catalyst, thus explaining the stability of BPA during catalysis in the dark. In the case of solar photolysis and catalysis in the dark, BPA degradation of about 20% was

1 observed after 45 min of treatment. In the CPC reactor, the borosilicate glass has a  
2 cut-off around 285 nm (Malato et al., 2009), however BPA is still photolyzed under  
3 solar irradiation at  $\lambda \geq 285$  nm since this range falls within the absorbance spectrum of  
4 BPA. The experiments in the CPC reactor were performed outdoors and the  
5 penetration of ambient light during catalysis in the dark was higher than in the batch  
6 reactors, which were placed indoors; a fact that explains the difference in BPA  
7 removal between the three systems as can be seen in Figure 4.

8 The effect of catalyst concentration on process efficiency was then investigated by  
9 applying various catalyst concentrations (100 – 500 mg/L) in order to remove 5 mg/L  
10 initial BPA concentration. In Figure 4, it is shown that increase of catalyst  
11 concentration from 100 to 250 mg/L improves significantly the removal of BPA in  
12 TiO<sub>2</sub>/UV-LED and TiO<sub>2</sub>/solar systems. For instance, the increase of TiO<sub>2</sub> from 100 to  
13 250 mg/L enhances BPA degradation by 21% and doubles the reaction rate (i.e. from  
14 0.040 to 0.080 min<sup>-1</sup>) in the CPC reactor (Figure 4c, Table 1). However, in TiO<sub>2</sub>/UV-  
15 BL system, a 4-fold increase of TiO<sub>2</sub> (i.e. from 125 to 500 mg/L) increases the  
16 reaction rate only by 1.5 times (i.e. from 0.013 to 0.018 min<sup>-1</sup>), resulting finally in  
17 64.8% BPA removal after 45 min of treatment [a percentage still much lower than  
18 those obtained by TiO<sub>2</sub>/UV-LED and TiO<sub>2</sub>/solar systems at the half TiO<sub>2</sub>  
19 concentration (i.e. 250 mg/L)]. In general, increase of TiO<sub>2</sub> concentration up to a  
20 point, where all catalyst particles are totally irradiated, enhances removal efficiency  
21 by offering more active sites for photocatalytic oxidation (Kaneco et al., 2004).  
22 However, this dependence is less profound in the case of TiO<sub>2</sub>/UV-BL system, which  
23 can be attributed to the lower light intensity emitted by the UV-BL lamp.

Figure 4. Control experiments and effect of catalyst concentration on photocatalytic degradation under (a) UV-LED, (b) UV-BL, and (c) solar irradiation ( $C_0 = 5 \text{ mg/L}$ ).

### 3.3 Mineralisation efficiency

The aim of photocatalytic oxidation is to destroy both parent compounds, and transformation products (TPs) formed during treatment. To this end, additional experiments were performed at the best-assayed conditions (i.e.  $C_0 = 2.5 \text{ mg/L}$ ,  $\text{TiO}_2 = 250 \text{ mg/L}$ ) to assess the mineralisation efficiency of the three photocatalytic systems. As can be seen in Figure 5, the mineralisation of BPA proceeds slower than BPA degradation, which is attributed to the fact that mineralisation includes a sequence of reactions for the oxidation of BPA and its TPs to  $\text{CO}_2$  and  $\text{H}_2\text{O}$ , thus taking longer than the partial oxidation of BPA. In detail, 99.9% of BPA is degraded within 20, 30, and 120 min under UV-LED, solar, and UV-BL irradiation, while the respective TOC removals after 90 min of treatment are 88, 67, and 33%.

Figure 5. BPA and TOC removal under UV-LED, UV-BL, and solar irradiation ( $C_0 = 2.5 \text{ mg/L}$ ,  $\text{TiO}_2 = 250 \text{ mg/L}$ ).

(Kondrakov et al., 2014) reported that the  $\text{TiO}_2$ -mediated photocatalytic oxidation of BPA is driven by photogenerated holes and hydroxyl radicals leading to the formation of seven TPs according to the mechanism illustrated in Figure 6. Briefly, BPA oxidation proceeds via hydroxylation yielding hydroxylated and oxidized TPs that are transformed into aliphatic alcohols, carboxylic acids, and aldehydes via ring-opening

1 and further oxidation reactions, before their complete mineralisation (Kondrakov et  
2 al., 2014; Repousi et al., 2017).

3  
4 Figure 6. Mechanism of BPA degradation by TiO<sub>2</sub>-mediated photocatalysis, adopted  
5 from (Kondrakov et al., 2014).

### 7 **3.4 Effect of water matrix**

8 Humic acids (HA) solution was used in order to resemble more realistic water and  
9 wastewater treatment conditions. HA typically found in surface waters, may interfere  
10 with the reactive oxygen species produced during photocatalytic oxidation reactions,  
11 and, thus affect the degradation yields. The concentration of HA in surface waters  
12 typically varies from 2 to 10 mg/L (Alrousan et al., 2009). Taking this into account, 5  
13 and 8 mg/L HA were added to the reactant mixture to examine the effect of water  
14 matrix on the photocatalytic removal of BPA. Noticeably, and as shown in Figure 7,  
15 the addition of HA has a detrimental effect on photocatalytic performance under both  
16 UV-LED and UV-BL irradiation. Removal efficiency substantially decreases with the  
17 increasing concentration of HA. For example, when the reactant mixture is spiked  
18 with 8 mg/L HA, BPA removal is suppressed by 77 and 67% under UV-LED and  
19 UV-BL irradiation, respectively (Figure 7a). The retardation effect of HA on process  
20 efficiency can be ascribed to: (i) the competitive adsorption of HA onto the active  
21 sites of TiO<sub>2</sub> that slows down oxidation either via hydroxyl radical ( $\cdot\text{OH}$ ) attack or  
22 through direct electron transfer between photogenerated holes ( $h_{\text{vb}}^+$ ) and target  
23 molecules (Selli et al., 1999), and (ii) the reduced light penetration in the solution  
24 (Antonopoulou et al., 2015).



Additional experiments were performed at 2.5 mg/L BPA in the presence of 250 mg/L TiO<sub>2</sub> in the CPC reactor. Likewise, the increase in HA concentration from 5 to 8 mg/L resulted in a gradual decrease of BPA degradation rate, as shown in Figure 7b. These results indicate that the retardation degree of photocatalytic oxidation depends strongly on the complexity of the water matrix. Reaction rate decreases with increasing complexity, therefore, degradation in real water samples (e.g. wastewater, surface water) is expected to be slower due to the presence of constituents that can act as hydroxyl radical scavengers (Zacharakis et al., 2013).

Figure 7. Photocatalytic removal of BPA in the presence of different concentrations of HA under (a) UV-LED and UV-BL and (b) solar irradiation ((a) C<sub>0</sub> = 5 mg/L, TiO<sub>2</sub> = 125 mg/L, (b) C<sub>0</sub> = 2.5 mg/L, TiO<sub>2</sub> = 250 mg/L).

### 3.5 Comparison of the three photocatalytic systems

It was observed that the LED-driven photocatalytic system achieved the highest oxidation reaction rates (Table 1) under all experimental conditions assayed, due to the increased light intensity provided by the UV-LED. Although UV-LED and UV-BL light sources are both driven by the same electrical power of 11 W and emit irradiation predominantly at 365 nm, their light intensities vary significantly. The intensity of UV-LED light is 1005 W/m<sup>2</sup>, whereas the light intensity of UV-BL is only 22.49 W/m<sup>2</sup>. This difference stems from the directionalities of the two light sources; UV-LED produces a directional beam of light so there is no leak of UV light outside the reactor, UV-BL lamp, to the contrary, emits light in all directions, therefore, a fraction of the photons is lost. However, the higher light intensity

provided by the UV-LED does not lead to the analogous improvement of the reaction rates. In fact, the  $k$  values obtained during LED-photocatalysis are only 4 – 9 times higher than UV-BL, thus suggesting the lower photonic efficiency of the TiO<sub>2</sub>/UV-LED system. This can be explained by the dependency of the reaction rate to light intensity: (i) at low light intensities, the rate of photocatalytic reaction increases linearly with the light intensity, (ii) at intermediate light intensities, reaction rate increases with the square foot of the light intensity because separation of electron-hole pairs competes with recombination, and (iii) at high light intensities, reaction rate becomes independent of the light intensity and mass transfer is the main limitation (Herrmann, 1999; Ollis et al., 1991). Therefore, the right balance should be set between removal efficiency of pollutants and energy requirements of the process in order to obtain sustainable and cost-efficient photocatalytic systems. Scaling-up LED-driven photocatalysis can increase the photonic efficiency of the process because the high rate of energy transfer provided by the UV-LED makes the system ideal for the treatment of large volumes of wastewater.

The consumption of electric energy,  $E_{EO}$ , in TiO<sub>2</sub>/UV-LED system was found to be significantly lower compared to TiO<sub>2</sub>/UV-BL (Figure 8), also suggesting the high sustainability of LED-photocatalysis. For instance, at the best-assayed conditions,  $E_{EO}$  has been estimated at 7.171 kWh/m<sup>3</sup>/order for TiO<sub>2</sub>/UV-LED system and 43.067 kWh/m<sup>3</sup>/order for TiO<sub>2</sub>/UV-BL. This 6-fold difference in  $E_{EO}$  values translates into higher treatment cost for the TiO<sub>2</sub>/UV-BL system, as well as increased environmental impact due to augmented CO<sub>2</sub> emissions and fossil depletion (Chatzisyneon et al., 2013). (Shie et al., 2008) and (Shie and Pai, 2010) also found that the photocatalytic degradation of indoor air pollutants (e.g. toluene, formaldehyde) under UV-LED irradiation is a process substantially more energy-efficient than using conventional

UV irradiation sources. At this point, it should be also mentioned that the use of conventional UV lamps further increases the environmental impact of the process due to the hazards related to the presence of mercury.

Figure 8. Electric energy per order ( $E_{EO}$ ) of TiO<sub>2</sub>/UV-LED and TiO<sub>2</sub>/UV-BL systems for the photocatalytic degradation of various initial concentrations of BPA (TiO<sub>2</sub> = 125 mg/L).

Comparing the three treatment systems, TiO<sub>2</sub>/solar delivers the second highest removal efficiency following TiO<sub>2</sub>/UV-LED (Table 1), which is due to the fact that TiO<sub>2</sub> is activated by solar light at  $\lambda < 380$  nm, which accounts for only about 5% of the solar spectrum. Solar photocatalysis results in higher degradation rates than TiO<sub>2</sub>/UV-BL system, which can be explained by the higher intensity of sunlight (i.e. 25 - 30 W/m<sup>2</sup> at  $\lambda < 400$  nm) than UV-BL (i.e. 22.5 W/m<sup>2</sup>), as well as the optimised geometry of CPC reactors.

The geometry of the photocatalytic reactors affects significantly process efficiency and this can be seen by the UV energy requirement,  $Q_{uv}$ , of the three systems. The  $Q_{uv}$ , at the best-assayed conditions, for the removal of 99% of BPA was estimated at 30.9 kJ/L, 4.2 kJ/L, and 3.54 kJ/L for TiO<sub>2</sub>/UV-LED, TiO<sub>2</sub>/UV-BL, and TiO<sub>2</sub>/solar system, respectively. TiO<sub>2</sub>/solar system requires the lowest UV energy under the studied conditions. Similar results have been reported by (Saggioro et al., 2014) and (Haranaka-Funai et al., 2017), who compared the photocatalytic performance of CPC and batch-operated reactors in the presence of TiO<sub>2</sub> suspensions. Solar CPC reactors have been already optimised and provide a high optical efficiency that allows the use

of direct and diffuse radiation (Saggioro et al., 2014). Meanwhile, LED photocatalysis is an emerging technology and the optimisation of LED reactors is still under investigation.

Overall, high degradation rates combined with significant advantages regarding process economy and environmental safety, make the TiO<sub>2</sub>/solar photocatalytic system ideal for water treatment applications in sun-rich areas. For areas with inadequate sunlight, the use of LEDs as irradiation source was found to be an appropriate alternative to conventional UV-BL lamps, leading to photocatalytic systems of increased performance, energy efficiency and environmental sustainability.

#### **4 Conclusions**

The degradation of bisphenol-A (BPA), a well-known endocrine disruptor, was investigated in three photocatalytic systems under various UVA irradiation sources, namely UV-LED, UV-BL lamp, and natural sunlight. The effect of key operating parameters, such as initial BPA, catalyst concentration, treatment time, and water matrix, on the photocatalytic performance of the three systems was assessed. LED-driven photocatalysis yielded the highest reaction rates, followed by TiO<sub>2</sub>/solar, and TiO<sub>2</sub>/UV-BL systems, under all experimental conditions assayed. UV energy requirements of the three systems was found to descend in the order: TiO<sub>2</sub>/solar < TiO<sub>2</sub>/UV-BL < TiO<sub>2</sub>/UV-LED, indicating the low photonic efficiency of the UV-LED system and, thus, highlighting the need for optimised LED photocatalytic reactors.

All in all, photocatalysis powered by either sunlight, a renewable energy, or LEDs, an energy efficient and environmentally friendly light source, features significant advantages regarding the overall sustainability of the process. The increased

performance and environmental safety of LED-photocatalysis make the process ideal for the removal of emerging micropollutants in areas where solar photocatalysis might not be feasible due to inadequate sunlight. LEDs could be also used as a backup irradiation source in solar photocatalytic systems during less sunny days or periods with increased influent loads (e.g. touristic periods). To this end, future work should focus on the evaluation of process efficiency in real secondary wastewater matrices with emerging micropollutants present at environmentally relevant concentrations. Also, economic and environmental impact assessment of LED-photocatalysis is necessary in order to establish the suitability of the process as a tertiary treatment step in WWTPs before further scale-up.

## **Acknowledgements**

Financial support from MINECO (CTM2013-44317-R and CTQ2017-83549-R) is gratefully acknowledged. The authors would also like to thank Dr John Fakidis from Li-Fi R&D Centre at the University of Edinburgh for the measurements of the spectral irradiance of UV-LED and UV-BL.

## **References**

- Alrousan, D.M.A., Dunlop, P.S.M., McMurray, T.A., Byrne, J.A., 2009. Photocatalytic inactivation of *E. coli* in surface water using immobilised nanoparticle TiO<sub>2</sub> films. *Water Res.* 43, 47-54.
- Antonopoulou, M., Skoutelis, C.G., Daikopoulos, C., Deligiannakis, Y., Konstantinou, I.K., 2015. Probing the photolytic–photocatalytic degradation mechanism of DEET in the presence of natural or synthetic humic macromolecules using molecular-scavenging techniques and EPR spectroscopy. *Journal of Environmental Chemical Engineering* 3, 3005-3014.
- Belgiorno, V., Rizzo, L., Fatta, D., Della Rocca, C., Lofrano, G., Nikolaou, A., Naddeo, V., Meric, S., 2007. Review on endocrine disrupting-emerging compounds in

1 urban wastewater: occurrence and removal by photocatalysis and ultrasonic  
2 irradiation for wastewater reuse. *Desalination* 215, 166-176.

3 Bolton, J.R., Bircher, K.G., Tumas, W., Tolman, C.A., 2001. Figures-of-merit for the  
4 technical development and application of advanced oxidation technologies for both  
5 electric- and solar-driven systems. *Pure Appl. Chem.* 73, 627-637.

6 Chatzisyneon, E., Foteinis, S., Mantzavinos, D., Tsoutsos, T., 2013. Life cycle  
7 assessment of advanced oxidation processes for olive mill wastewater treatment.  
8 *Journal of Cleaner Production* 54, 229-234.

9 Dalrymple, O.K., Yeh, D.H., Trotz, M.A., 2007. Removing pharmaceuticals and  
10 endocrine-disrupting compounds from wastewater by photocatalysis. *Journal of*  
11 *Chemical Technology & Biotechnology* 82, 121-134.

12 Davididou, K., McRitchie, C., Antonopoulou, M., Konstantinou, I., Chatzisyneon, E.,  
13 2018. Photocatalytic degradation of saccharin under UV-LED and blacklight  
14 irradiation. *Journal of Chemical Technology & Biotechnology* 93, 269-276.

15 Deblonde, T., Cossu-Leguille, C., Hartemann, P., 2011. Emerging pollutants in  
16 wastewater: A review of the literature. *Int. J. Hyg. Environ. Health* 214, 442-448.

17 Dimitrakopoulou, D., Rethemiotaki, I., Frontistis, Z., Xekoukoulotakis, N.P., Venieri,  
18 D., Mantzavinos, D., 2012. Degradation, mineralization and antibiotic inactivation of  
19 amoxicillin by UV-A/TiO<sub>2</sub> photocatalysis. *J. Environ. Manage.* 98, 168-174.

20 Flint, S., Markle, T., Thompson, S., Wallace, E., 2012. Bisphenol A exposure, effects,  
21 and policy: A wildlife perspective. *J. Environ. Manage.* 104, 19-34.

22 Frontistis, Z., Daskalaki, V.M., Katsaounis, A., Poullos, I., Mantzavinos, D., 2011.  
23 Electrochemical enhancement of solar photocatalysis: Degradation of endocrine  
24 disruptor bisphenol-A on Ti/TiO<sub>2</sub> films. *Water Res.* 45, 2996-3004.

25 Giulivo, M., Lopez de Alda, M., Capri, E., Barceló, D., 2016. Human exposure to  
26 endocrine disrupting compounds: Their role in reproductive systems, metabolic  
27 syndrome and breast cancer. A review. *Environ. Res.* 151, 251-264.

28 Haranaka-Funai, D., Didier, F., Giménez, J., Marco, P., Esplugas, S., Machulek-  
29 Junior, A., 2017. Photocatalytic treatment of valproic acid sodium salt with TiO<sub>2</sub> in  
30 different experimental devices: An economic and energetic comparison. *Chem. Eng.*  
31 *J.* 327, 656-665.

32 Herrmann, J.-M., 1999. Heterogeneous photocatalysis: fundamentals and applications  
33 to the removal of various types of aqueous pollutants. *Catal. Today* 53, 115-129.

34 Jo, W.-K., Tayade, R.J., 2014. New Generation Energy-Efficient Light Source for  
35 Photocatalysis: LEDs for Environmental Applications. *Industrial & Engineering*  
36 *Chemistry Research* 53, 2073-2084.

37 Kaneco, S., Rahman, M.A., Suzuki, T., Katsumata, H., Ohta, K., 2004. Optimization  
38 of solar photocatalytic degradation conditions of bisphenol A in water using titanium  
39 dioxide. *Journal of Photochemistry and Photobiology A: Chemistry* 163, 419-424.

- 1 Kasprzyk-Hordern, B., Dinsdale, R.M., Guwy, A.J., 2009. The removal of  
2 pharmaceuticals, personal care products, endocrine disruptors and illicit drugs during  
3 wastewater treatment and its impact on the quality of receiving waters. *Water Res.* 43,  
4 363-380.
- 5 Kleywegt, S., Pileggi, V., Yang, P., Hao, C., Zhao, X., Rocks, C., Thach, S., Cheung,  
6 P., Whitehead, B., 2011. Pharmaceuticals, hormones and bisphenol A in untreated  
7 source and finished drinking water in Ontario, Canada — Occurrence and treatment  
8 efficiency. *Sci. Total Environ.* 409, 1481-1488.
- 9 Kondrakov, A.O., Ignatev, A.N., Frimmel, F.H., Bräse, S., Horn, H., Revelsky, A.I.,  
10 2014. Formation of genotoxic quinones during bisphenol A degradation by TiO<sub>2</sub>  
11 photocatalysis and UV photolysis: A comparative study. *Applied Catalysis B:  
12 Environmental* 160–161, 106-114.
- 13 Legrini, O., Oliveros, E., Braun, A.M., 1993. Photochemical processes for water  
14 treatment. *Chem. Rev.* 93, 671-698.
- 15 Li, D.K., Zhou, Z., Miao, M., He, Y., Qing, D., Wu, T., Wang, J., Weng, X., Ferber,  
16 J., Herrinton, L.J., Zhu, Q., Gao, E., Yuan, W., 2010. Relationship Between Urine  
17 Bisphenol-A Level and Declining Male Sexual Function. *Journal of Andrology* 31,  
18 500-506.
- 19 Loos, R., Locoro, G., Comero, S., Contini, S., Schwesig, D., Werres, F., Balsaa, P.,  
20 Gans, O., Weiss, S., Blaha, L., Bolchi, M., Gawlik, B.M., 2010. Pan-European survey  
21 on the occurrence of selected polar organic persistent pollutants in ground water.  
22 *Water Res.* 44, 4115-4126.
- 23 Luo, Y., Guo, W., Ngo, H.H., Nghiem, L.D., Hai, F.I., Zhang, J., Liang, S., Wang,  
24 X.C., 2014. A review on the occurrence of micropollutants in the aquatic environment  
25 and their fate and removal during wastewater treatment. *Sci. Total Environ.* 473-474,  
26 619-641.
- 27 Mahamuni, N.N., Adewuyi, Y.G., 2010. Advanced oxidation processes (AOPs)  
28 involving ultrasound for waste water treatment: A review with emphasis on cost  
29 estimation. *Ultrason. Sonochem.* 17, 990-1003.
- 30 Malato, S., Fernández-Ibáñez, P., Maldonado, M.I., Blanco, J., Gernjak, W., 2009.  
31 Decontamination and disinfection of water by solar photocatalysis: Recent overview  
32 and trends. *Catal. Today* 147, 1-59.
- 33 Matafonova, G., Batoev, V., 2018. Recent advances in application of UV light-  
34 emitting diodes for degrading organic pollutants in water through advanced oxidation  
35 processes: A review. *Water Res.* 132, 177-189.
- 36 Meeker, J.D., Ehrlich, S., Toth, T.L., Wright, D.L., Calafat, A.M., Trisini, A.T., Ye,  
37 X., Hauser, R., 2010. Semen quality and sperm DNA damage in relation to urinary  
38 bisphenol A among men from an infertility clinic. *Reprod. Toxicol.* 30, 532-539.
- 39 Ollis, D.F., Pelizzetti, E., Serpone, N., 1991. Photocatalyzed destruction of water  
40 contaminants. *Environ. Sci. Technol.* 25, 1522-1529.

- 1 Repousi, V., Petala, A., Frontistis, Z., Antonopoulou, M., Konstantinou, I.,  
2 Kondarides, D.I., Mantzavinos, D., 2017. Photocatalytic degradation of bisphenol A  
3 over Rh/TiO<sub>2</sub> suspensions in different water matrices. *Catal. Today* 284, 59-66.
- 4 Rubin, B.S., 2011. Bisphenol A: An endocrine disruptor with widespread exposure  
5 and multiple effects. *The Journal of Steroid Biochemistry and Molecular Biology* 127,  
6 27-34.
- 7 Saggiaro, E.M., Oliveira, A.S., Pavesi, T., Tototzintle, M.J., Maldonado, M.I.,  
8 Correia, F.V., Moreira, J.C., 2014. Solar CPC pilot plant photocatalytic degradation of  
9 bisphenol A in waters and wastewaters using suspended and supported-TiO<sub>2</sub>.  
10 Influence of photogenerated species. *Environmental Science and Pollution Research*  
11 21, 12112-12121.
- 12 Selli, E., Baglio, D., Montanarella, L., Bidoglio, G., 1999. Role of humic acids in the  
13 TiO<sub>2</sub>-photocatalyzed degradation of tetrachloroethene in water. *Water Res.* 33, 1827-  
14 1836.
- 15 Shie, J.-L., Lee, C.-H., Chiou, C.-S., Chang, C.-T., Chang, C.-C., Chang, C.-Y., 2008.  
16 Photodegradation kinetics of formaldehyde using light sources of UVA, UVC and  
17 UVLED in the presence of composed silver titanium oxide photocatalyst. *J. Hazard.*  
18 *Mater.* 155, 164-172.
- 19 Shie, J.-L., Pai, C.-Y., 2010. Photodegradation Kinetics of Toluene in Indoor Air at  
20 Different Humidities Using UVA, UVC and UVLED Light Sources in the Presence of  
21 Silver Titanium Dioxide. *Indoor Built Environ.* 19, 503-512.
- 22 Subagio, D.P., Srinivasan, M., Lim, M., Lim, T.-T., 2010. Photocatalytic degradation  
23 of bisphenol-A by nitrogen-doped TiO<sub>2</sub> hollow sphere in a vis-LED photoreactor.  
24 *Applied Catalysis B: Environmental* 95, 414-422.
- 25 Tokode, O., Prabhu, R., Lawton, L., Robertson, P.J., 2015. UV LED Sources for  
26 Heterogeneous Photocatalysis, in: Bahnemann, D.W., Robertson, P.K.J. (Eds.),  
27 *Environmental Photochemistry Part III*. Springer Berlin Heidelberg, pp. 159-179.
- 28 Tsai, W.-T., Lee, M.-K., Su, T.-Y., Chang, Y.-M., 2009. Photodegradation of  
29 bisphenol-A in a batch TiO<sub>2</sub> suspension reactor. *J. Hazard. Mater.* 168, 269-275.
- 30 Tsonev, D., Videv, S., Haas, H., 2015. Towards a 100 Gb/s visible light wireless  
31 access network. *Opt. Express* 23, 1627-1637.
- 32 Zacharakis, A., Chatzisyneon, E., Binas, V., Frontistis, Z., Venieri, D., Mantzavinos,  
33 D., 2013. Solar Photocatalytic Degradation of Bisphenol A on Immobilized ZnO or  
34 TiO<sub>2</sub>. *International Journal of Photoenergy* 2013, 9.
- 35 Zhang, C., Li, Y., Wang, C., Niu, L., Cai, W., 2016. Occurrence of endocrine  
36 disrupting compounds in aqueous environment and their bacterial degradation: A  
37 review. *Crit. Rev. Environ. Sci. Technol.* 46, 1-59.

38



1  
2  
3  
4  
5  
6  
7  
8  
9  
10  
11  
12  
13  
14  
15  
16  
17  
18  
19

**List of Tables**

Table 1. Removal percentages (R), pseudo-first-order kinetic constants ( $k$ ), and coefficients of linear regression of data fitting ( $r^2$ ) for the photocatalytic degradation of BPA under UV-LED, UV-BL, and solar irradiation.

1

2

3

4

5

6 Table 1.

Operating parameter	Irradiation source	mg/L	R, %	Pseudo-first-order reaction model	
				$k$ , min <sup>-1</sup>	$r^2$
$C_0^a$	UV-LED	2.5	99.9	0.179	1.00
		5	95.9	0.058	1.00
		7.5	90.6	0.047	0.98
		10	79.7	0.036	0.99
	UV-BL	2.5	66.8	0.021	0.98
		5	45.6	0.013	0.97
		7.5	36.0	0.011	0.99
		10	29.5	0.007	0.98
	Solar	2.5	99.9	0.132	0.95
		5	84.0	0.047	0.93
		7.5	81.5	0.037	0.90
		10	72.9	0.035	0.98
$TiO_2^b$	UV-LED	100	97.9	0.068	0.99
		125	95.9	0.057	1.00
		250	99.0	0.101	1.00
	UV-BL	125	45.6	0.013	0.97
		250	57.5	0.016	0.97
		500	64.8	0.018	0.99
	Solar	100	79.0	0.040	0.99
		125	84.0	0.047	0.93
		250	99.9	0.080	0.97
Best-assayed operating conditions <sup>c</sup>	UV-LED		99.9	0.230	0.99
	UV-BL		75.6	0.025	0.98
	Solar		99.9	0.151	0.98

7 <sup>a</sup>TiO<sub>2</sub> = 125 mg/L, irradiation time = 45 min;

<sup>b</sup> $C_0 = 5 \text{ mg/L}$ , irradiation time = 45 min;

<sup>c</sup> $C_0 = 2.5 \text{ mg/L}$ ,  $\text{TiO}_2 = 250 \text{ mg/L}$ , irradiation time = 45 min.

3

4

5

## 6 **List of Figures**

7 Figure 1. Schematics of (a) UV-LED, (b) UV-BL, and (c) solar CPC reactors.

8 Figure 2. The relative spectral irradiance of UV-LED and UV-BL irradiation sources  
9 and the action spectra of  $\text{TiO}_2$  P25 catalyst (in grey).

10 Figure 3. Effect of initial BPA concentration on photocatalytic degradation under (a)  
11 UV-LED, (b) UV-BL, and (c) solar irradiation. Inset graphs: relationship between  
12 reaction rate constant and initial BPA concentration ( $\text{TiO}_2 = 125 \text{ mg/L}$ ).

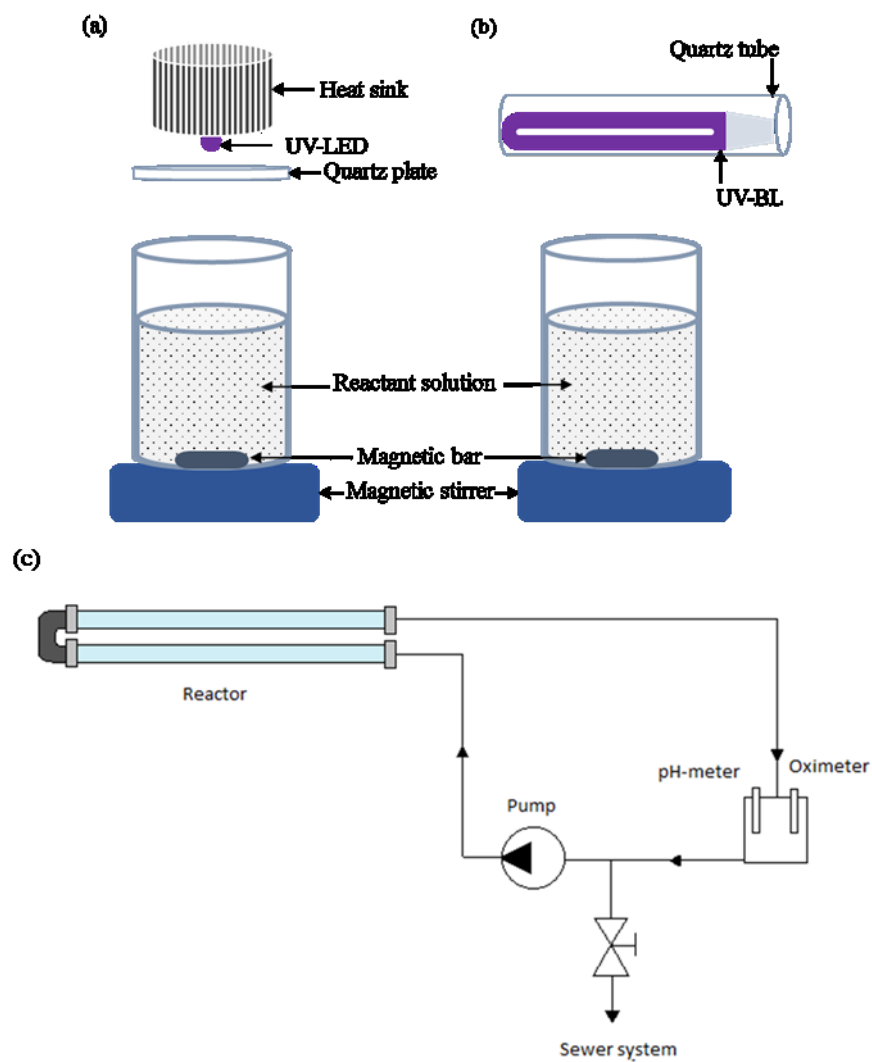
13 Figure 4. Control experiments and effect of catalyst concentration on photocatalytic  
14 degradation under (a) UV-LED, (b) UV-BL, and (c) solar irradiation ( $C_0 = 5 \text{ mg/L}$ ).

15 Figure 5. BPA and TOC removal under UV-LED, UV-BL, and solar irradiation ( $C_0 =$   
16  $2.5 \text{ mg/L}$ ,  $\text{TiO}_2 = 250 \text{ mg/L}$ ).

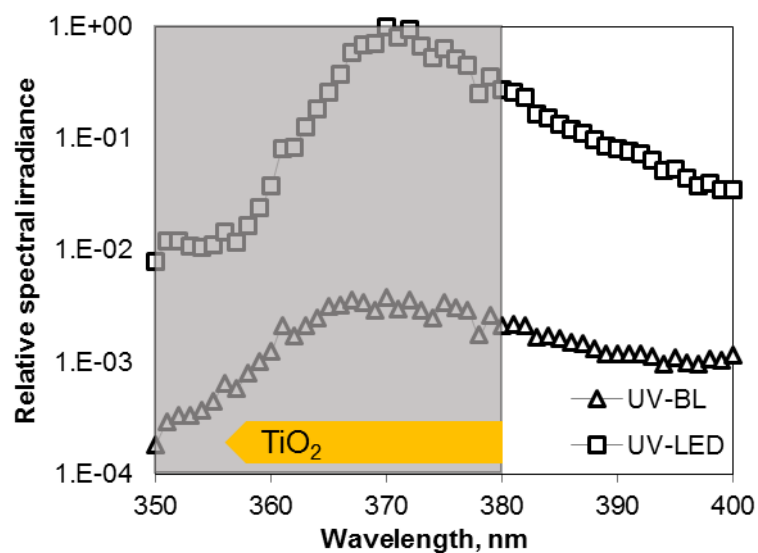
17 Figure 6. Mechanism of BPA degradation by  $\text{TiO}_2$ -mediated photocatalysis, adopted  
18 from (Kondrakov et al., 2014).

19 Figure 7. Photocatalytic removal of BPA in the presence of different concentrations of  
20 HA under (a) UV-LED and UV-BL and (b) solar irradiation ((a)  $C_0 = 5 \text{ mg/L}$ ,  $\text{TiO}_2 =$   
21  $125 \text{ mg/L}$ , (b)  $C_0 = 2.5 \text{ mg/L}$ ,  $\text{TiO}_2 = 250 \text{ mg/L}$ ).

1 Figure 8. Electric energy per order ( $E_{EO}$ ) for  $\text{TiO}_2$ /UV-LED and  $\text{TiO}_2$ /UV-BL systems  
 2 for the photocatalytic degradation of different initial concentrations of BPA ( $\text{TiO}_2$  =  
 3 125 mg/L).



7  
 8 Figure 1. Schematics of (a) UV-LED, (b) UV-BL, and (c) solar CPC reactors.



1

2 Figure 2. The relative spectral irradiance of UV-LED and UV-BL irradiation sources  
 3 and the action spectra of TiO<sub>2</sub> P25 catalyst (in grey).

4

5

6

7

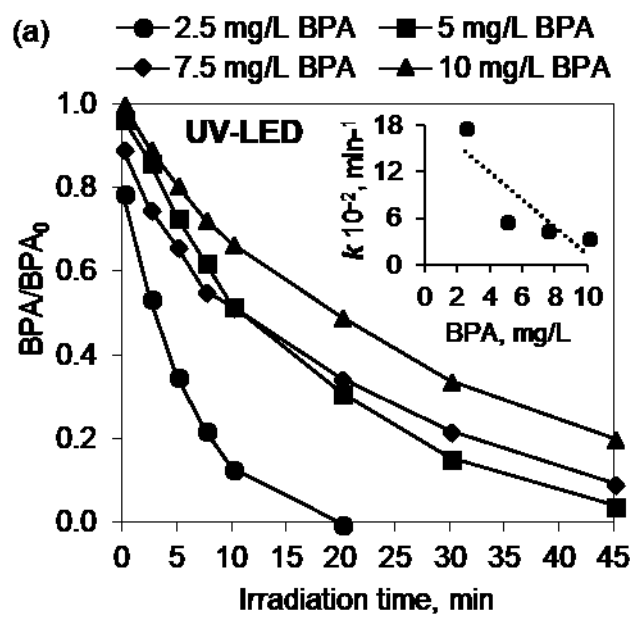
8

9

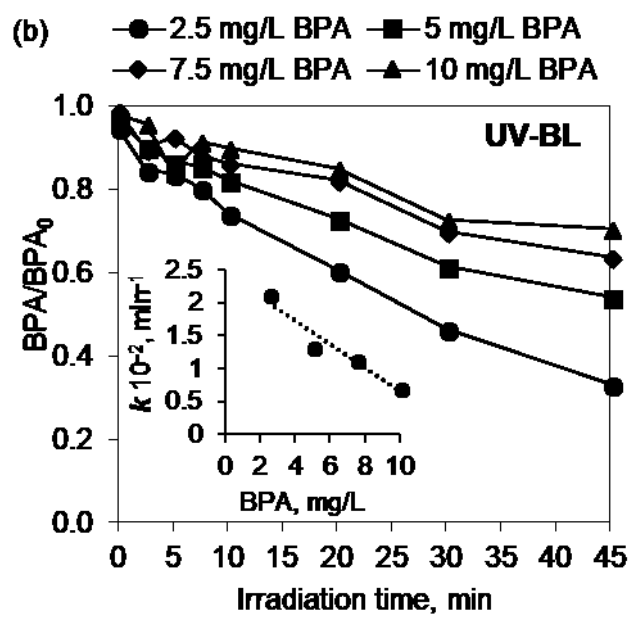
10

11

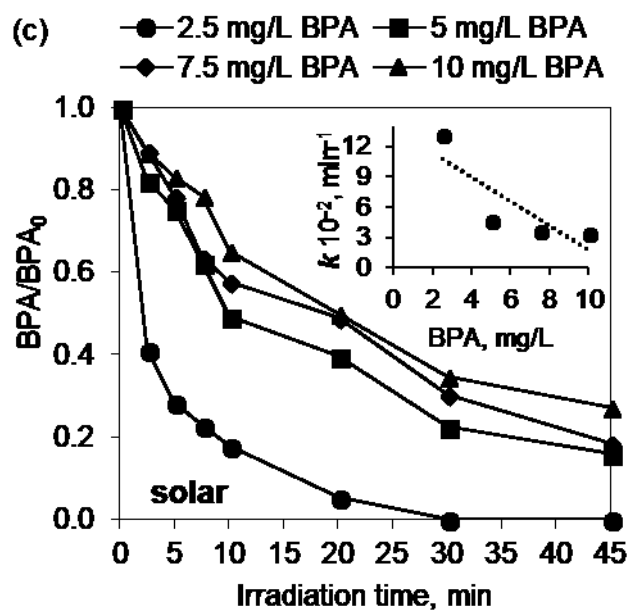
12



1



2



1

2 Figure 3. Effect of initial BPA concentration on photocatalytic degradation under (a)  
 3 UV-LED, (b) UV-BL, and (c) solar irradiation. Inset graphs: relationship between  
 4 reaction rate constant and initial BPA concentration ( $TiO_2 = 125 \text{ mg/L}$ ).

5

6

7

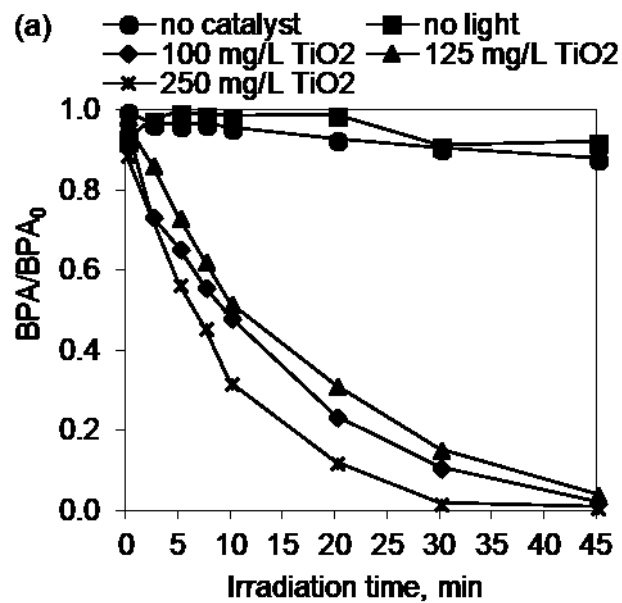
8

9

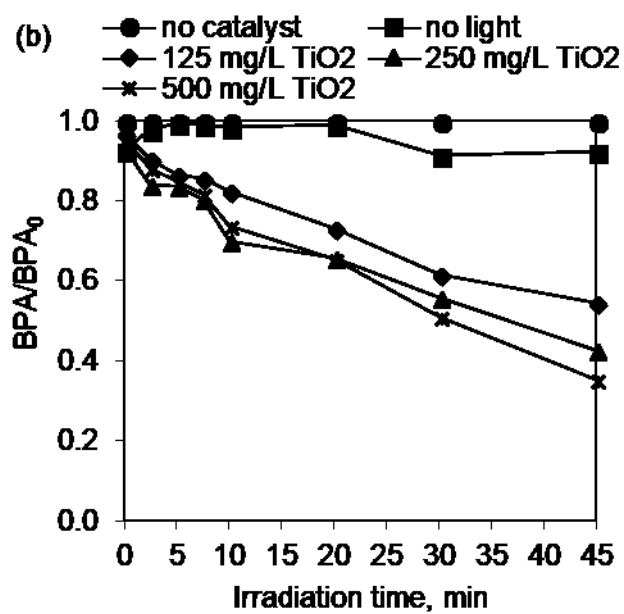
10

11

12

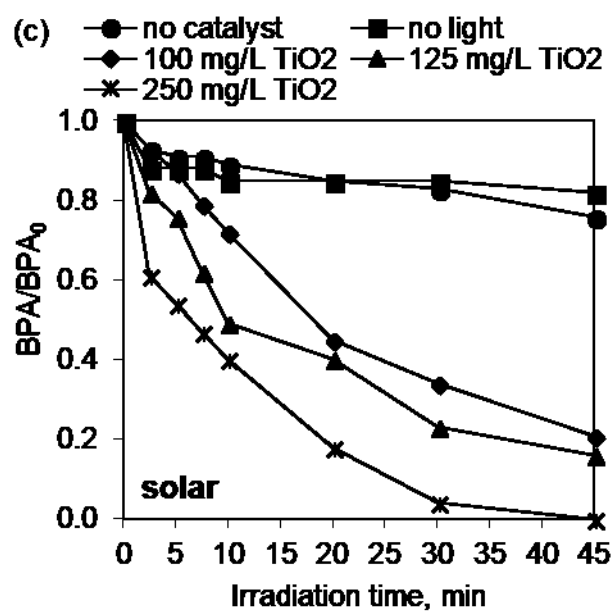


1



2





1

2 Figure 4. Control experiments and effect of catalyst concentration on photocatalytic  
3 degradation under (a) UV-LED, (b) UV-BL, and (c) solar irradiation ( $C_0 = 5$  mg/L).

4

5

6

7

8

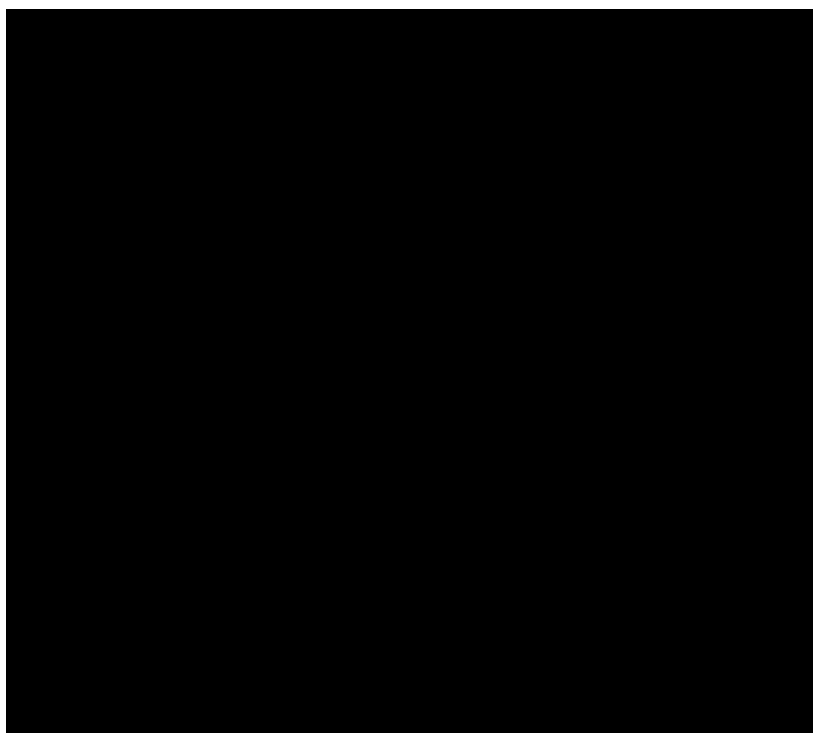
9

10

11

12

13



1

2 Figure 5. BPA and TOC removal under UV-LED, UV-BL, and solar irradiation ( $C_0 =$   
3 2.5 mg/L,  $TiO_2 = 250$  mg/L).

4

5

6

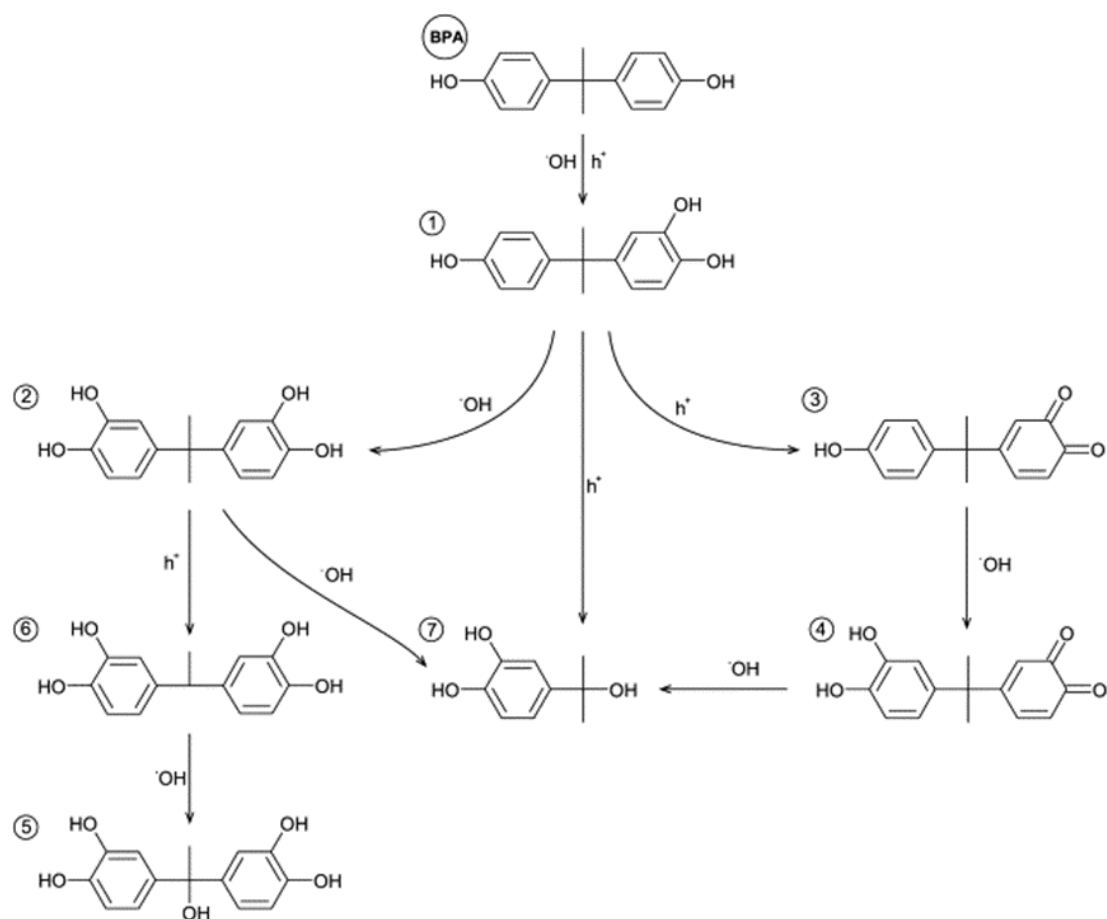
7

8

9

10

11



1

2 Figure 6. Mechanism of BPA degradation by TiO<sub>2</sub>-mediated photocatalysis, adopted  
 3 from (Kondrakov et al., 2014).

4

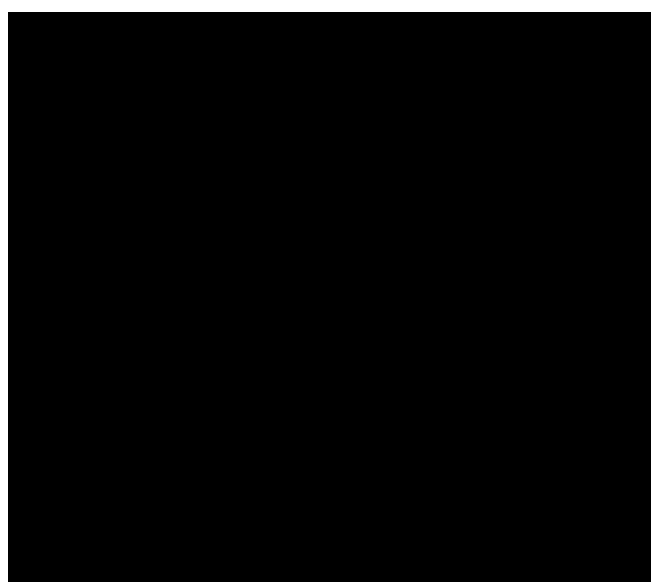
5

6

7

8

9



1

2

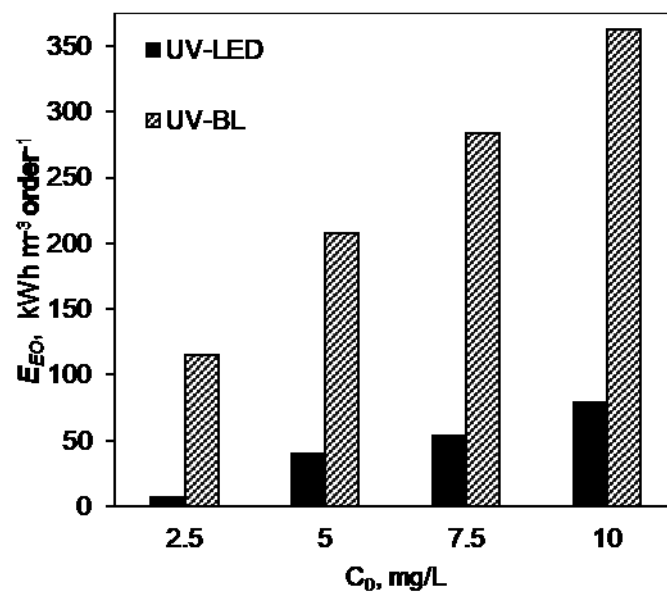
3 Figure 7. Photocatalytic removal of BPA in the presence of different concentrations of  
 4 HA under (a) UV-LED and UV-BL and (b) solar irradiation ((a)  $C_0 = 5$  mg/L,  $\text{TiO}_2 =$   
 5  $125$  mg/L, (b)  $C_0 = 2.5$  mg/L,  $\text{TiO}_2 = 250$  mg/L).

6

7

8

9



1

2 Figure 8. Electric energy per order ( $E_{EO}$ ) of TiO<sub>2</sub>/UV-LED and TiO<sub>2</sub>/UV-BL systems  
 3 for the photocatalytic degradation of different initial concentrations of BPA (TiO<sub>2</sub> =  
 4 125 mg/L).

5